

Reflective Optical Fiber Sensors Based on Tilted Fiber Bragg Gratings Fabricated With Femtosecond Laser

Chao Chen, Yong-Sen Yu, Rui Yang, Chuang Wang, Jing-Chun Guo, Yang Xue, Qi-Dai Chen, and Hong-Bo Sun, *Member, IEEE*

Abstract—The fabrication of tilted fiber Bragg gratings (TFBGs) in non-photosensitized single-mode fiber by infrared femtosecond (fs) laser is reported for the first time to the best of our knowledge. The tilted grating structure is obtained by focusing laser pulses through a phase mask into a tilted positioned fiber sample, which is moving along with the interference fringe to form a grating region covering the entire fiber core and partial cladding. A reflective fiber probe based on the TFBG with a gold mirror sputtered on one end has been fabricated and its maximum refractive index (RI) sensitivity is 12.276 nm/RI unit in the RI range of 1.4091–1.4230 for the cladding mode LP020. A wavelength-power demodulated technique based on the sensors has been proposed to measure axial strain and temperature simultaneously, which is found suited to work in harsh environment, especially at high temperature up to 800° C.

Index Terms—Femtosecond (fs) laser, optical fiber sensors, tilted fiber Bragg gratings (TFBGs).

I. INTRODUCTION

RECENTLY, tilted fiber Bragg gratings (TFBGs) have been considered as the important components in novel fiber sensors [1]–[6] because they have the sensing characteristics of both uniform fiber Bragg gratings (FBGs) and long period fiber gratings (LPFGs) [7]. In the TFBGs, light coupling occurs not only between the forward and backward core modes but also between the forward core mode and backward cladding modes and even radiation modes [8]. The conventional method to fabricate FBGs is using an ultraviolet (UV) excimer laser source [1]–[7]. The UV-written gratings are dependent on the fiber intrinsic photosensitivity and the induced refractive index (RI) modulation is limited by the saturation effect. In addition, the regular grating structures are easy to erase when temperature is higher than 400° C [9] unless a high temperature annealing regenerated process is applied to the gratings [10]. To solve these problems, the femtosecond (fs) laser microfabrication technique has been adopted in recent years [11], [12]. The grating formation result from the permanent breakage of the covalent bonds due to the strong nonlinear interaction between

the glass and fs laser. In this case, photosensitization, including hydrogen-loading or increasing germanium-doping level, is no more needed and the grating structures are high temperature stable. Furthermore, the nonlinear light absorption induces a relative strong local RI modulation, which will increase additional propagation loss, but ensures that the length of the fs-written FBG is short, a smaller grating length reduces the spatial averaging of surrounding RI, which could increase the measurement accuracy, making it an ideal fiber sensor in fixed point measurement. However, to the best of our knowledge, the fabrication of fiber gratings by fs laser has only been studied in uniform- [11]–[14], chirped- [15], [16], sampled- [17], [18], and phase shifted-FBGs [18] and LPFGs [19], [20]. To date, there have no reports on the fs-written TFBGs.

In this paper, we demonstrated, for the first time, the fabrication of TFBGs in non-photosensitized single-mode fiber (SMF) by infrared fs laser. The phase mask method is adopted in our experiment [11]–[13]. The tilted grating planes in the fiber is constructed by moving the fiber sample, which is rotated a little tilt angle relative to the focal line, along with the interference fringe. In addition, a gold mirror is sputtered on the cleaved fiber end with 40 mm apart from the grating region to form a reflective fiber probe with reflective configuration [1], which is significant in narrow region detection and remote monitoring. The surrounding RI sensitivity of the TFBG probe has been tested through the resonant wavelength of the cladding mode LP020 and the maximum RI-sensitivity is 12.276 nm/RI unit (RIU) in the RI range of 1.4091–1.4230. Moreover, we propose a wavelength-power demodulation method to realize the simultaneous measurement of axial strain and temperature at high temperature, extending the temperature measurement range compared with the method of using differential response of the core mode and cladding modes to the parameters of the external environment [1], [21], [22].

II. EXPERIMENTS

The experimental layout for fabrication of TFBGs is shown in Fig. 1. A Ti: sapphire regenerative amplifier laser system (Spectra Physics) with the operation wavelength of $\lambda_{\text{in}} = 800$ nm and 100 fs pulse duration was adopted. The 2.5 mm radius (ω_0) with 0.45 mJ pulse energy at 100 Hz repetition rate was focused using a cylindrical lens (focal length, 40 mm) through a phase mask (pitch, 3.33 μm) into the fiber (Corning SMF-28). The phase mask was positioned 3 mm away from the fiber to generate pure interference between the ± 1 st-order diffractive

Manuscript received August 27, 2012; revised November 07, 2012; accepted December 03, 2012. Date of publication December 12, 2012; date of current version January 09, 2013. This work was supported by the National Natural Science Foundation of China under Grant 91123027 and Grant 90923037.

The authors are with State Key Laboratory on Integrated Optoelectronics, College of Electronic Science and Engineering, Jilin University, Changchun 130012, China (e-mail: yuys@jlu.edu.cn; hbsun@jlu.edu.cn).

Color versions of one or more of the figures in this paper are available online at <http://ieeexplore.ieee.org>.

Digital Object Identifier 10.1109/JLT.2012.2232643

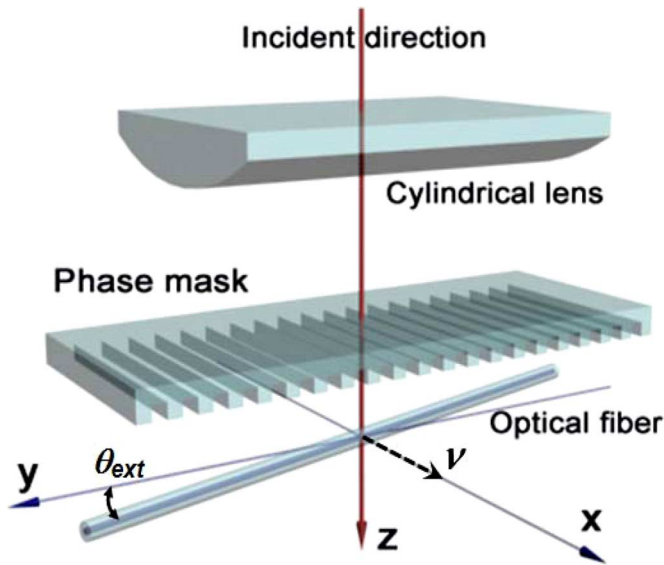


Fig. 1. Experimental layout for the fs laser fabrication of TFBGs.

laser beams [23]. The average light power intensity in the focal line was about $7.3 \times 10^{12} \text{ W/cm}^2$. In the fabrication process, the fiber was rotated with a tilt angle of θ_{ext} relative to the focal line, which is parallel to the y axis as shown in Fig. 1. Because the focal line width ($\omega \approx \lambda_{\text{in}} f / \pi \omega_0 \approx 4 \mu\text{m}$) was less than the fiber core diameter ($8.3 \mu\text{m}$), the fiber was moving along with the interference fringe, parallel to the x axis [Fig. 1], with a velocity of $1 \mu\text{m/s}$ to obtain the tilted RI modulation in entire fiber core and partial cladding. The spectrum of the TFBG was monitored by an optical spectrum analyzer (OSA) (AQ6370B, Yokogawa) with the resolution of 0.02 nm and a broadband light source (Superk Compact, NKT Photonics).

The TFBG probe was realized through gold sputtering on the cleaved fiber end apart from the grating region. The gold sputtering process was implemented in a small ion sputtering instrument (JEOL, JFC-1600) with the current of 20 mA and the absolute vacuum degree of 9 Pa . After 10 minutes sputtering, a gold layer with a thickness of 30 nm was achieved to form a broadband reflector. The thickness was measured by an atomic force microscopy (AFM). The schematic diagram of the TFBG probe is shown in Fig. 2(a). The light in the fiber core passes through the grating region twice due to the broadband reflector at the fiber end, resulting in a double loss of the resonant cladding modes [1].

The fs-written TFBGs with different tilt angles were fabricated as shown in Fig. 2(b)–(d). The TFBG with a tilt angle of 4° was chosen to demonstrate the characteristics. Its transmission spectra with different order number are shown in Fig. 3. The top and bottom spectra are the 3rd- and 4th-order Bragg resonant peaks, and their corresponding discrete cladding modes resonances, respectively. The length of grating region is just 3.6 mm , shorter than that of the traditional UV-TFBGs (about 10 mm), and the length could be much shorter if necessary. But the spectral profiles only have a depth of $\sim 4 \text{ dB}$, indicating a relative small refractive index modulation and coupling coefficient. The reasons maybe: firstly, in the grating fabrication process, the cylindrical lens and the optical fiber are not parallel and thus

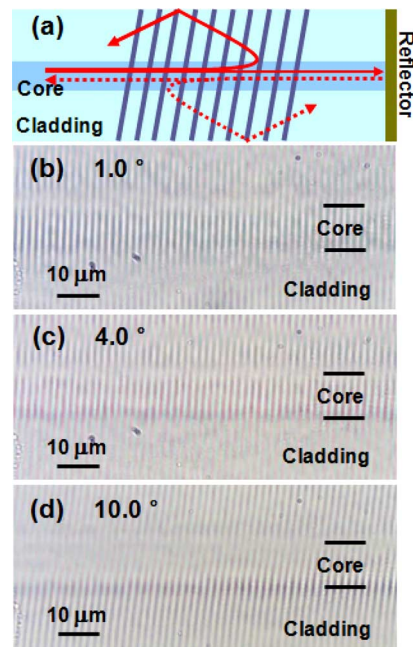


Fig. 2. (a) Schematic diagram of the fs-written TFBG probe with reflective configuration. (b)–(d) Microscopic images of the fs laser induced grating structures with different tilt angles.

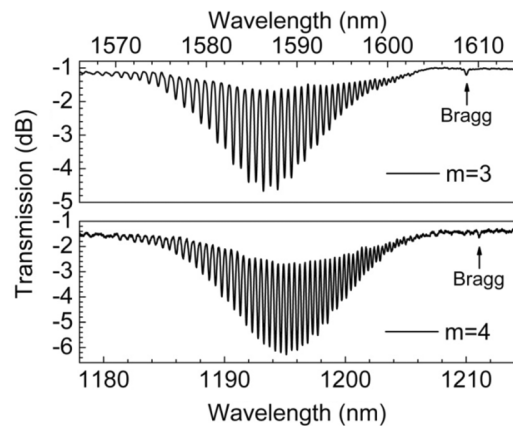


Fig. 3. The transmission spectra of the fs-written TFBG with a tilt angle of 4° .

form a distorted optical system to form the grating planes by interference inside the fiber, decreasing the fringe visibility. In addition, the grating structure extending to part of the cladding is likely to impact the modes coupling and thus suppress the cladding mode resonance amplitude. Subsequently, a smooth fiber end away from the tilted grating region was cleaved and a gold mirror was sputtered on it to form the TFBG probe. The probe size, namely the length from the fiber end to the grating region, is customized according to the practical requirements. In this work, the distance between the reflector and grating region was designed relative long with the length of 40 mm in order to test the characteristics of the axial strain. The reflection spectrum of the TFBG probe is shown in Fig. 4, represented by the red curve. The resonances of Bragg and cladding modes appear as peak and a series of troughs, and the amplitudes of the cladding modes resonant peaks are twice larger than that in

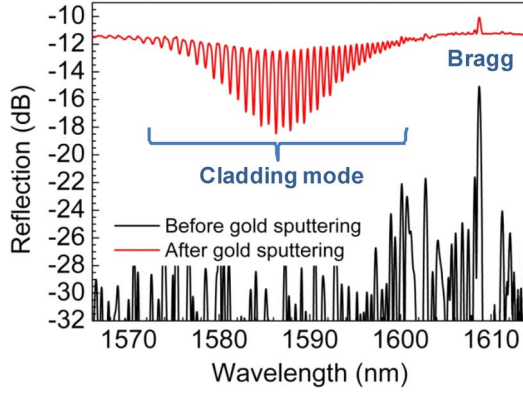


Fig. 4. The reflection spectra of the fs-written TFBG sensor before (black line) and after (red line) gold sputtering.

transmission spectrum [Fig. 3, top figure]. The reflection spectrum before gold sputtering is also shown in Fig. 4 to compare with the sputtered one. Before the sensing tests, the TFBG probe was pre-annealing 8 hours at 400° C to erase the unstable RI modulation [12], [24], ensuring a stable spectrum in repeated temperature measurements.

In the TFBGs, the effective modes coupling needs to meet two requirements. One is the phase match condition, which determines the resonant wavelength. The formulas are as follows [7], [8]

$$m\lambda_B = 2n_{\text{eff,core}}(\lambda_B)\Lambda_g \quad (1)$$

$$m\lambda_{\text{clad}}^{\nu\mu} = \left(n_{\text{eff,core}}(\lambda_{\text{clad}}^{\nu\mu}) + n_{\text{eff,clad}}(\lambda_{\text{clad}}^{\nu\mu}) \right) \Lambda_g \quad (2)$$

where $\Lambda_g = \Lambda/\cos\theta$ is the fiber axial projection of the grating period Λ with the tilt angle of θ , $n_{\text{eff,core}}(\lambda_B)$ is the effective RI of the core mode at the Bragg resonant wavelength λ_B , $n_{\text{eff,core}}(\lambda_{\text{clad}}^{\nu\mu})$ and $n_{\text{eff,clad}}(\lambda_{\text{clad}}^{\nu\mu})$ are the effective RIs of the core and cladding modes at the resonant wavelength of cladding mode $\lambda_{\text{clad}}^{\nu\mu}$, m is the Bragg diffractive order number. The other condition is that the overlap of the coupling modes are sufficient enough to obtain a significant coupling coefficient [8], which decides the coupling strength and the amplitude of the resonant peak. The characteristics of the TFBGs' spectra and sensing are primarily determined by the two conditions.

III. SENSING CHARACTERISTICS AND RESULTS

A. Refractive Index Sensing Characteristics

The TFBG sensor was immersed in different concentrations of glycerin water solutions to test its surrounding RI sensing characteristics [Fig. 5]. The RI range of the glycerin water solutions was 1.331–1.4608, which were collimated by an Abbe refractometer at room temperature (20° C). After each measurement, the sensor was cleaned with ethanol and deionized water to recover its original spectrum in air for the next test. The reflection spectrum changes with surrounding RI as shown in Fig. 5(a). The supported cladding modes become radiative when the refractive index of the surrounding becomes comparable to effective index [1], [2], [7], [8].

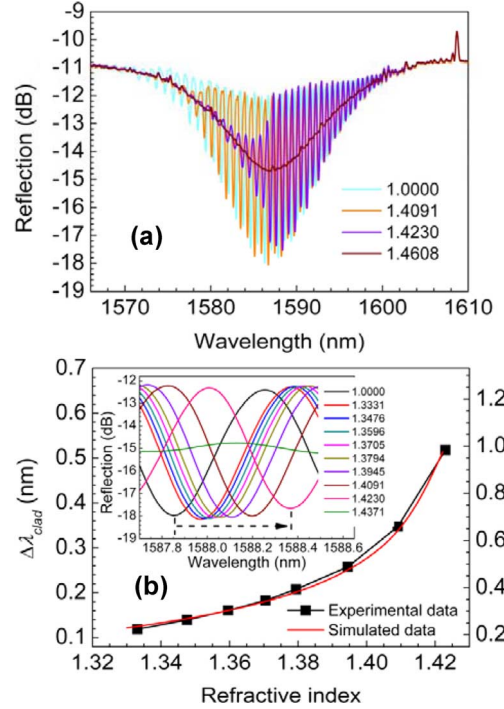


Fig. 5. (a) The evolution of the reflection spectrum versus the surrounding RI for the fs-written TFBGs sensor. (b) Variation of the resonance wavelength and the effective RI of cladding mode LP020 as a function of the surrounding RI, the inset shows cladding mode LP020 resonances versus the surrounding RI.

To analyze the RI sensitivity of the TFBGs, there are two main methods. One is relate to light power calculated by integral of the spectral area [2], [7], the other is to monitor the wavelength change [1], [21], [25]. The latter is adopted in our experiment due to its simpleness and high accuracy, and the results are shown in Fig. 5(b). The inset figure is the RI response of the cladding mode LP020 with the resonant wavelength of 1587.86 nm. The resonant wavelength change ($\Delta\lambda_{\text{clad}}^{020}$) with surrounding RI is shown in the main figure, represented by black squares. The simulated results (red curve) calculated by formula (2) are also plotted and they are in agreement with the experiments. Furthermore, the calculated effective RI changes of the cladding mode in different environments are shown at the right side y-axis. The RI sensitivity has an obvious increase when the surrounding RI is close to the RI value of the cladding mode cut-off. The maximum RI sensitivity is 12.276 nm/RIU in the RI range of 1.4091–1.4230 for the cladding mode LP020. Higher RI sensitivity can also be obtained through monitoring the higher-order cladding mode resonance, but the dynamic range will be narrowed. Moreover, the RI sensitivity could be increased easily to hundreds of nm/RIU by putting a thin gold coating on the fiber, exciting the surface plasmonic resonance [3], [26], [27]. In RI measurement, the temperature cross-sensitivity could be eliminated by the differential response of Bragg and cladding modes resonances [25].

B. Axial Strain and Temperature Sensing Characteristics

In addition to the surrounding RI measurement, axial strain and temperature sensing of the TFBG probe were also carried out. The resonant wavelength shift ($\Delta\lambda_{\text{clad}}^{020}$, $\Delta\lambda_B$) of

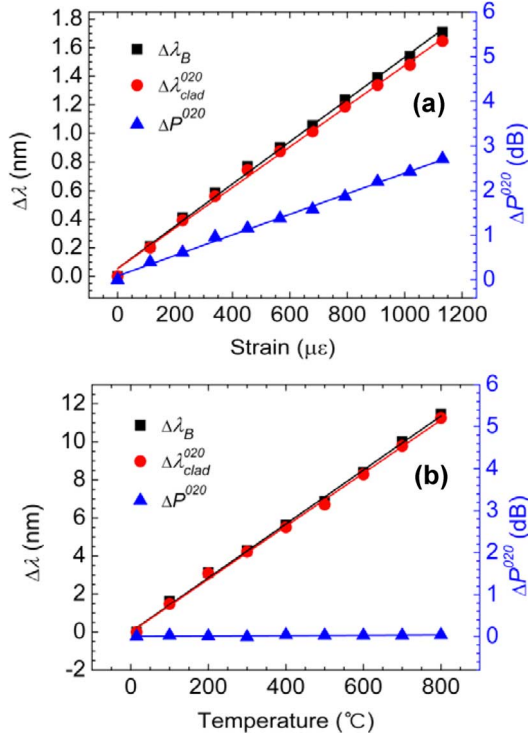


Fig. 6. (a) Variation of $\Delta\lambda_B$, $\Delta\lambda_{\text{clad}}^{020}$ and ΔP^{020} versus the axial strain for the reflective fs-written TFBGs sensor. (b) Variation of $\Delta\lambda_B$, $\Delta\lambda_{\text{clad}}^{020}$ and ΔP^{020} versus the temperature.

cladding mode LP020 and Bragg resonance and the change of their peaks power difference (relative peaks power change, $\Delta(P_B - P_{\text{clad}}^{\nu\mu}) = \Delta P^{\nu\mu}$) are functions of the axial strain and temperature, which are shown in Fig. 6. The measurement of strain response was realized through adding axial tension to the TFBG. The axial strain inside the fiber was calculated by equation $\epsilon = F/\pi r^2 E$, where F is the axial tension, r is the cladding radius, and E is the silica Young's modulus. Fig. 6(a) shows the change of axial strain not only results in the resonant wavelength shift, but also affects the relative peaks power. The strain sensitivities of wavelength and power are 1.48 pm/ $\mu\epsilon$, 1.42 pm/ $\mu\epsilon$, and 2.3×10^{-3} dB/ $\mu\epsilon$, respectively, corresponding to λ_B , $\lambda_{\text{clad}}^{020}$, and P^{020} . The differential response of the resonances of Bragg and cladding mode becomes notable with the axial strain increasing.

The results of temperature response of $\Delta\lambda_B$, $\Delta\lambda_{\text{clad}}^{020}$ and ΔP^{020} , respectively, from room temperature to 800°C are shown in Fig. 6(b). When the temperature is below 300°C, the temperature dependence of cladding mode resonance is similar to that of the Bragg resonance, while their response to temperature are different for temperature higher than 300°C. The temperature has no impact on the relative peaks power [Fig. 6(b)]. The temperature sensitivities of λ_B , $\lambda_{\text{clad}}^{020}$, and P^{020} are 14.2 pm/°C, 13.9 pm/°C, and 0 dB/°C, respectively, by linear fitting in Fig. 6(b).

According to the experimental results, $\Delta P^{\nu\mu}$ is independent of temperature and strongly dependent on stress. This behavior is mainly due to the two reasons as below. Firstly, the axial strain is likely to impact on the extinction ratio of the grating fringe, namely the refractive index modulation, resulting in the change

of $\Delta P^{\nu\mu}$. Secondly, the axial strain varies the grating modified region, which is mainly related to the scattering loss, leading to the variation of $\Delta P^{\nu\mu}$. For the temperature characteristics of silica fiber, the thermal-expansion coefficient is one order of magnitude smaller than the thermal-optic coefficient. So the thermal-expansion induced elastic-optic effect can be considered very weak, leading to a tiny axial strain, which is difficult to affect the $\Delta P^{\nu\mu}$.

Here we propose a method based on the resonant wavelength and relative peaks power, namely wavelength-power demodulated technique, to realize the simultaneous measurement of axial strain and temperature from room temperature to 800°C. This method allows a much better strain-temperature discrimination than using the small strain sensitivity difference between the core and cladding modes [1], [22]. The relationship between these variables can be expressed in the form of matrix

$$\begin{pmatrix} \Delta\lambda_B \\ \Delta P^{\nu\mu} \end{pmatrix} = \begin{pmatrix} k_{B,\epsilon} & k_{B,T} \\ k_{p,\epsilon}^{\nu\mu} & k_{p,T}^{\nu\mu} \end{pmatrix} \begin{pmatrix} \Delta\epsilon \\ \Delta T \end{pmatrix} = \mathbf{K} \begin{pmatrix} \Delta\epsilon \\ \Delta T \end{pmatrix} \quad (3)$$

where $k_{B,\epsilon}$ and $k_{p,\epsilon}^{\nu\mu}$ are the axial strain sensitivities of the Bragg resonant wavelength and relative peaks power, respectively, $k_{B,T}$ and $k_{p,T}^{\nu\mu}$ are the corresponding temperature sensitivities. Substituting the values obtained from experiments into the matrix, the change of axial strain and temperature is written as

$$\begin{pmatrix} \Delta\epsilon \\ \Delta T \end{pmatrix} = \begin{pmatrix} 1.48 & 14.2 \\ 0.0023 & 0 \end{pmatrix}^{-1} \begin{pmatrix} \Delta\lambda_B \\ \Delta P^{020} \end{pmatrix} \quad (4)$$

The experimental results are affected by the measurement errors of $\Delta\lambda_B$ and $\Delta P^{\nu\mu}$, represented by $\delta(\Delta\lambda_B)$ and $\delta(\Delta P^{\nu\mu})$, and their response to environment fluctuations induced nonlinear error $\delta\mathbf{K}$. The measurement tolerances of strain and temperature can be obtained through the equation as follows [28]

$$\begin{pmatrix} \delta(\Delta\epsilon) \\ \delta(\Delta T) \end{pmatrix} = (\mathbf{K}_0 + \delta\mathbf{K})^{-1} \begin{pmatrix} \Delta\lambda_{B,0} + \delta(\Delta\lambda_B) \\ \Delta P_0^{\nu\mu} + \delta(\Delta P^{\nu\mu}) \end{pmatrix} - \mathbf{K}_0^{-1} \begin{pmatrix} \Delta\lambda_{B,0} \\ \Delta P_0^{\nu\mu} \end{pmatrix} \quad (5)$$

where \mathbf{K}_0 , $\Delta\lambda_{B,0}$ and $\Delta P_0^{\nu\mu}$ are the true values of \mathbf{K} , $\Delta\lambda_B$ and $\Delta P^{\nu\mu}$, respectively. $\delta(\Delta\lambda_B)$ and $\delta(\Delta P^{\nu\mu})$ are determined by the OSA's wavelength and power resolutions, which are 0.02 nm and 0.05 dBm, respectively, and the bandwidth of the resonant peaks. According to the (5), the maximum measurement errors of strain and temperature are estimated to 11.4 $\mu\epsilon$ and 4.7°C, respectively.

The simultaneous sensing of temperature and axial strain can also be implemented through integral of spectrum area instead of relative peaks power, but the method needs some complex calculation and is not simple as the method proposed in this paper.

IV. CONCLUSION

In conclusion, we have fabricated TFBGs in non-photosensitized SMF by infrared fs laser for the first time. An fs-written TFBG with the length of 3.6 mm and a tilt angle of 4° has been obtained through moving the tilted fiber along with the

interference fringe behind a phase mask. The TFBG sensing probe is realized by gold mirror sputtered on the cleaved fiber end with 40 mm apart from the grating region. The probe size can be customized according to practical requirements. Sensing characteristics of the reflective TFBG probe for surrounding RI, axial strain and temperature have been studied. A two-parameter demodulation method based on wavelength and power difference is proposed for simultaneous measurement of axial strain and temperature, even at high temperature up to 800°C. This fs-written TFBGs have all the advantages already demonstrated for UV-TFBGs and additional ones such as high temperature stability (inherent in fs-written gratings), a better strain-temperature discrimination because of the strain induced resonance amplitudes changes, and the availability of multiple order resonances from a single grating. The fs-written TFBG probe has potential applications in chemical and physical sensing fields, especially in high temperature harsh environment.

REFERENCES

- [1] C. F. Chan, C. Chen, A. Jafari, A. Laronche, D. J. Thomson, and J. Albert, "Optical fiber refractometer using narrowband cladding-mode resonance shifts," *Appl. Opt.*, vol. 46, no. 7, pp. 1142–1149, Mar. 2007.
- [2] N. J. Alberto, C. A. Marques, J. L. Pinto, and R. N. Nogueira, "Three-parameter optical fiber sensor based on a tilted fiber Bragg grating," *Appl. Opt.*, vol. 49, no. 31, pp. 6085–6091, Nov. 2010.
- [3] Y. Y. Shevchenko and J. Albert, "Plasmon resonances in gold-coated tilted fiber Bragg gratings," *Opt. Lett.*, vol. 32, no. 3, pp. 211–213, Feb. 2007.
- [4] A. C. L. Wong, W. H. Chung, H. Y. Tam, and C. Lu, "Single tilted Bragg reflector fiber laser for simultaneous sensing of refractive index and temperature," *Opt. Exp.*, vol. 19, no. 2, pp. 409–414, Jan. 2011.
- [5] B. Zhou, A. P. Zhang, S. He, and B. Gu, "Cladding-mode-recoupling-based tilted fiber Bragg grating sensor with a core-diameter-mismatched fiber section," *IEEE Photon. J.*, vol. 2, no. 2, pp. 152–157, Apr. 2010.
- [6] G. E. Villanueva, M. B. Jakubinek, B. Simard, C. J. Oton, J. Matres, L. Y. Shao, P. P. Millán, and J. Albert, "Linear and nonlinear optical properties of carbon nanotube-coated single-mode optical fiber gratings," *Opt. Lett.*, vol. 36, no. 11, pp. 2104–2106, June 2011.
- [7] G. Laffont and P. Ferdinand, "Tilted short-period fibre-Bragg-grating-induced coupling to cladding modes for accurate refractometry," *Meas. Sci. Technol.*, vol. 12, no. 7, pp. 765–770, July 2001.
- [8] T. Erdogan and J. E. Sipe, "Tilted fiber phase gratings," *J. Opt. Soc. Amer. A*, vol. 13, no. 2, pp. 296–313, Feb. 1996.
- [9] J. Rathje, M. Kristensen, and J. E. Pedersen, "Continuous anneal method for characterizing the thermal stability of ultraviolet Bragg gratings," *J. Appl. Phys.*, vol. 88, pp. 1050–1055, July 2000.
- [10] S. Bandyopadhyay, J. Canning, M. Stevenson, and K. Cook, "Ultra-high-temperature regenerated gratings in boron-codoped germanosilicate optical fiber using 193 nm," *Opt. Lett.*, vol. 33, no. 16, pp. 1917–1919, Aug. 2008.
- [11] S. J. Mihailov, C. W. Smelser, P. Lu, R. B. Walker, D. Grobncic, H. Ding, G. Henderson, and J. Unruh, "Fiber Bragg gratings made with a phase mask and 800-nm femtosecond radiation," *Opt. Lett.*, vol. 28, no. 12, pp. 995–997, Jun. 2003.
- [12] C. Chen, Y. S. Yu, R. Yang, L. Wang, J. C. Guo, Q. D. Chen, and H. B. Sun, "Monitoring thermal effect in femtosecond laser interaction with glass by fiber Bragg grating," *J. Lightw. Technol.*, vol. 29, no. 14, pp. 2126–2130, Jul. 2011.
- [13] R. Yang, Y. S. Yu, C. Chen, Q. D. Chen, and H. B. Sun, "Rapid fabrication of microhole array structured optical fibers," *Opt. Lett.*, vol. 36, no. 19, pp. 3879–3881, Oct. 2011.
- [14] S. J. Mihailov, D. Grobncic, C. W. Smelser, P. Lu, R. B. Walker, and H. Ding, "Bragg grating inscription in various optical fibers with femtosecond infrared lasers and a phase mask," *Opt. Mater. Express.*, vol. 1, no. 4, pp. 754–765, Aug. 2011.
- [15] J. Thomas, C. Voigtländer, D. Schimpf, F. Stutzki, E. Wikszak, J. Limpert, S. Nolte, and A. Tünnermann, "Continuously chirped fiber Bragg gratings by femtosecond laser structuring," *Opt. Lett.*, vol. 33, no. 14, pp. 1560–1562, July 2008.
- [16] C. Voigtländer, J. Thomas, E. Wikszak, P. Dannberg, S. Nolte, and A. Tünnermann, "Chirped fiber Bragg gratings written with ultrashort pulses and a tunable phase mask," *Opt. Lett.*, vol. 34, no. 12, pp. 1888–1890, June 2009.
- [17] X. Fang, X. Y. He, C. R. Liao, M. Yang, D. N. Wang, and Y. Wang, "A new method for sampled fiber Bragg grating fabrication by use of both femtosecond laser and CO₂ laser," *Opt. Exp.*, vol. 18, no. 3, pp. 2646–2654, Feb. 2010.
- [18] G. D. Marshall, R. J. Williams, N. Jovanovic, M. J. Steel, and M. J. Withford, "Point-by-point written fiber-Bragg gratings and their application in complex grating designs," *Opt. Exp.*, vol. 18, no. 19, pp. 19844–19859, Sept. 2010.
- [19] Y. Kondo, K. Nouchi, T. Mitsuyu, M. Watanabe, P. G. Kazansky, and K. Hirao, "Fabrication of long-period fiber gratings by focused irradiation of infrared femtosecond laser pulses," *Opt. Lett.*, vol. 24, no. 10, pp. 646–648, May 1999.
- [20] J. C. Guo, Y. S. Yu, X. L. Zhang, C. Chen, R. Yang, C. Wang, R. Z. Yang, Q. D. Chen, and H. B. Sun, "Compact long-period fiber gratings with resonance at second-order diffraction," *IEEE Photon. Technol. Lett.*, vol. 24, no. 16, pp. 1393–1395, May 2012.
- [21] E. Chehura, S. W. James, and R. P. Tatam, "Temperature and strain discrimination using a single tilted fibre Bragg grating," *Opt. Commun.*, vol. 275, pp. 344–347, Mar. 2007.
- [22] C. Chen and J. Albert, "Strain-optic coefficients of the individual cladding modes of a single mode fiber: Theory and experiment," *Electron. Lett.*, vol. 42, no. 18, pp. 2027–2028, Aug. 2006.
- [23] C. W. Smelser, D. Grobncic, and S. J. Mihailov, "Generation of pure two-beam interference grating structures in an optical fiber with a femtosecond infrared source and a phase mask," *Opt. Lett.*, vol. 29, no. 15, pp. 1730–1732, Aug. 2004.
- [24] C. W. Smelser, S. J. Mihailov, and D. Grobncic, "Formation of type I-IR and type II-IR gratings with an ultrafast IR laser and a phase mask," *Opt. Exp.*, vol. 13, no. 14, pp. 5377–5386, Jul. 2005.
- [25] C. Chen, C. Caucheteur, P. Megret, and J. Albert, "The sensitivity characteristics of tilted fibre Bragg grating sensors with different cladding thicknesses," *Meas. Sci. Technol.*, vol. 18, no. 10, pp. 3117–3122, Oct. 2007.
- [26] Y. Shevchenko, C. Chen, M. A. Dakka, and J. Albert, "Polarization-selective grating excitation of plasmons in cylindrical optical fibers," *Opt. Lett.*, vol. 35, no. 5, pp. 637–639, Mar. 2010.
- [27] C. Caucheteur, Y. Shevchenko, L. Y. Shao, M. Wuilpart, and J. Albert, "High resolution interrogation of tilted fiber grating SPR sensors from polarization properties measurement," *Opt. Exp.*, vol. 19, no. 2, pp. 1656–1664, Jan. 2011.
- [28] W. Jin, W. C. Michie, G. Thursby, M. Konstantaki, and B. Culshaw, "Simultaneous measurement of strain and temperature: Error analysis," *Opt. Eng.*, vol. 36, no. 2, pp. 598–609, Feb. 1997.

Chao Chen received the B.S. and the M.S. degrees in electronics science and technology from the College of Electronic Science and Engineering, Jilin University, Changchun, China, in 2005 and 2010, respectively. He is currently pursuing the Ph.D. degree in the College of Electronic Science and Engineering, Jilin University.

His current research interests include design and femtosecond laser fabrication of fiber gratings, and fiber optic sensors. From July 2005 to Aug. 2007, he worked as an engineer in Ibiden Electronics (Beijing) Co. Ltd.

Yong-Sen Yu received the M.S. degree in electronics from Changchun University of Science and Technology, Changchun, China, in 2000, and the Ph.D. degree in the College of Electronic Science and Engineering from Jilin University, Changchun, China, in 2005.

In 2009, he worked as an Associate Professor in State Key Lab of Integrated Optoelectronics, Jilin University, Changchun, China. His current research interests include laser microfabrication, fiber gratings, and fiber optic sensors.

Rui Yang received the B.S. degree in microelectronics from the College of Electronic Science and Engineering, Jilin University, Changchun, China, in 2009. He is currently pursuing the Ph.D. degree in the College of Electronic Science and Engineering, Jilin University.

His current research interests include femtosecond laser fabrication of fiber gratings and fiber optic sensors.

Chuang Wang received the B.S. degree in electronics science and technology from the College of Electronic Science and Engineering, Jilin University, Changchun, China, in 2008. He is currently pursuing the M. S. degree in the College of Electronic Science and Engineering, Jilin University.

His current research interests include femtosecond laser fabrication of fiber gratings and fiber optic sensors.

Jing-Chun Guo received the B.S. degree in applied physics from the College of Physics, Jilin University, Changchun, China, in 2010. He is currently pursuing the M.S. degree in the College of Electronic Science and Engineering, Jilin University.

His current research interests include femtosecond laser fabrication of fiber gratings and fiber optic sensors.

Yang Xue received the B.S. degree in electronics science and technology from the College of Electronic Science and Engineering, Jilin University, Changchun, China, in 2011. He is currently pursuing the M. S. degree in the College of Electronic Science and Engineering, Jilin University. His current research interests include femtosecond laser fabrication of fiber gratings and fiber optic sensors.

Qi-Dai Chen received the B.S. degree in physics from the University of Science and Technology of China, Hefei, China, in 1998, and the Ph.D. degree in the Institute of Physics, Chinese Academy of Sciences, Beijing, China, in 2004.

He was doing post-doctorate research at Osaka City University during 2005–2006. He is an Associate Professor with Jilin University. His current research interests include laser microfabrication, ultrafast laser spectroscopy, photochemistry, and photophysics.

Hong-Bo Sun received the B.S. and the Ph.D. degrees in electronics from Jilin University, Changchun, China, in 1992 and 1996, respectively.

He worked as a Postdoctoral Researcher in Satellite Venture Business Laboratory, University of Tokushima, Japan, from 1996 to 2000, and then as an Assistant Professor in the Department of Applied Physics, Osaka University, Osaka, Japan. In 2005, he was promoted as a Full Professor (Changjiang Scholar), Jilin University, China. His research interests have been laser nanofabrication and ultrafast spectroscopy: Fabrication of various micro-optical, microelectronic, micromechanical, microoptoelectronic, microfluidic components and integrated systems at nanoscales, and exploring ultrafast dynamics of photons, electrons, phonons, and surface plasmons in solar cells, organic light-emitting devices and low-dimensional quantum systems at femtosecond timescale. So far, he has published nearly 150 scientific papers in the above fields, which have been cited nearly 5000 times according to ISI search report.